

Coordinated Photoinduced Electron and Proton Transfer in a Molecular Triad

Su-Chun Hung, Alisdair N. Macpherson, Su Lin, Paul A. Liddell, Gilbert R. Seely, Ana L. Moore,* Thomas A. Moore,* and Devens Gust*

Department of Chemistry and Biochemistry
Center for the Study of Early Events in Photosynthesis
Arizona State University, Tempe, Arizona 85287-1604

Received November 11, 1994

Excitation of carotenoid–porphyrin–quinone (C–P–Q) triads yields the porphyrin first excited singlet state, which decays by electron transfer to give a C–P⁺–Q^{•-} charge-separated state. Competing with rapid charge recombination is electron transfer from the carotenoid to produce a long-lived C⁺–P–Q^{•-} species. High quantum yields of the final state require tuning of electronic and thermodynamic factors to favor forward electron transfer over charge recombination.^{1,2} Triad 1 illustrates a new strategy for slowing charge recombination based on coupling photoinduced electron transfer to a change in proton chemical potential. The naphthoquinone moiety of 1 is fused to a norbornene system bearing a carboxylic acid at a bridgehead so that an intramolecular hydrogen bond from the carboxyl group to the nearby quinone carbonyl can form.³ Electron transfer from the photoexcited porphyrin results in a marked pK_a increase at the quinone,⁴ leading to a proton shift from the acid that generates a new state with a reduced recombination rate. The result is a 2-fold gain in quantum yield of the final charge-separated state relative to reference triads 2 and 3.

The absorption spectra of compounds 1–6⁸ are unperturbed relative to those of models, indicating that interchromophore interactions are weak. Although the fluorescence emissions of 1–6 have the same band shape and energy as those of a model porphyrin, the quantum yields are sharply reduced due to electron transfer to the naphthoquinone, which shortens the singlet lifetime relative to the ~10 ns lifetime for a model porphyrin.⁹ The decay-associated fluorescence spectrum for 2, a triad which cannot undergo intramolecular hydrogen bonding, features one main component of 55 ps. Two significant fluorescence decay components were found for 1. The major component (51 ps, 69%) is assigned to triads with an intramolecular hydrogen bond, and the minor, 157-ps decay (23%) is attributed to a population lacking this bond.^{10,11} Triad 2 was

(1) Gust, D.; Moore, T. A.; Moore, A. L. *Acc. Chem. Res.* **1993**, *26*, 198–205. Gust, D.; Moore, T. A.; Moore, A. L.; Macpherson, A. N.; Lopez, A.; DeGraziano, J. M.; Gouni, I.; Bittersmann, E.; Seely, G. R.; Gao, F.; Nieman, R. A.; Ma, X. C.; Demanche, L.; Luttrull, D. K.; Lee, S.-J.; Kerrigan, P. K. *J. Am. Chem. Soc.* **1993**, *115*, 11141–11152. Moore, T. A.; Gust, D.; Hatlevig, S.; Moore, A. L.; Makings, L. R.; Pessiki, P. J.; De Schryver, F. C.; Van der Auweraer, M.; Lexa, D.; Bensasson, R. V.; Rougée, M. *Isr. J. Chem.* **1988**, *28*, 87–95.

(2) Wasielewski, M. R. *Chem. Rev.* **1992**, *92*, 435–461.

(3) FT-IR spectra of the quinone model of 1 (1-carboxy-1,2,3,4-tetrahydro-1,4-methanoanthracene-9,10-dione) in dichloromethane (0.004 M) provide evidence for intramolecular hydrogen bonding. Quinone carbonyl stretching bands are observed at 1665 (not hydrogen bonded) and 1630 cm⁻¹ (internally hydrogen bonded), indicating an equilibrium mixture of the two forms. The acid carbonyl stretch occurs at 1748 and is accompanied by a 1713-cm⁻¹ band at concentrations greater than or equal to 0.01 M due to intermolecular hydrogen bonding.

(4) The pK_a of protonated ketones is approximately -7, and those of semiquinones are typically ~3–5.⁵ The pK_a of protonated lawsone is -5.6,⁶ and that of the semiquinone is 4.7.⁷

(5) Neta, P. In *The Chemistry of Quinonoid Compounds*; Patai, S., Rappoport, Z., Eds.; Wiley: New York, 1988; Vol. 2, Part 2, p 886.

(6) Beauchamp, A.; Benoit, R. R. *Can. J. Chem.* **1966**, *44*, 1607–1613.

(7) Rao, P. S.; Hayon, E. *J. Phys. Chem.* **1973**, *77*, 2274–2276.

(8) NMR and mass spectrometric data for all compounds were consistent with the proposed structures. Synthetic details will be reported elsewhere.

(9) Hung, S.-C.; Lin, S.; Macpherson, A. N.; DeGraziano, J. M.; Kerrigan, P. K.; Liddell, P. A.; Moore, A. L.; Moore, T. A.; Gust, D. *J. Photochem. Photobiol. A: Chem.* **1994**, *77*, 207–216.

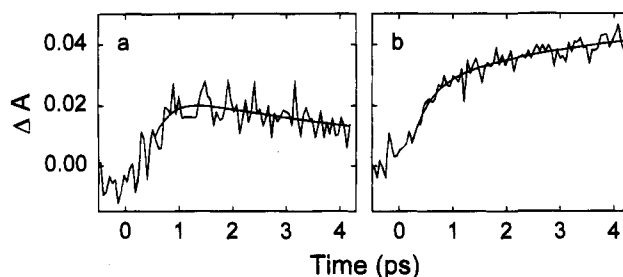


Figure 1. (a) Rise of the transient absorption at 660–662 nm of dyad 5 in benzonitrile solution following excitation at 590 nm with ~200-fs laser flashes. The fit shown yields a 250-fs rise time. (b) Similar transient for dyad 4 fitted with rise times of 350 fs and 3.8 ps.

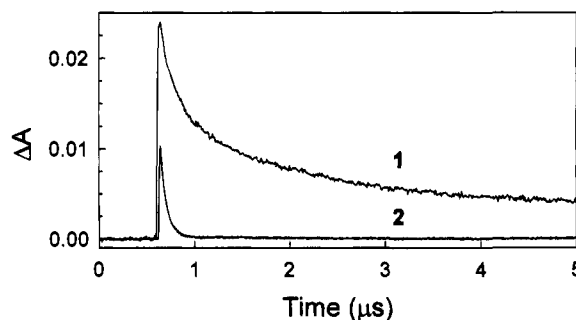
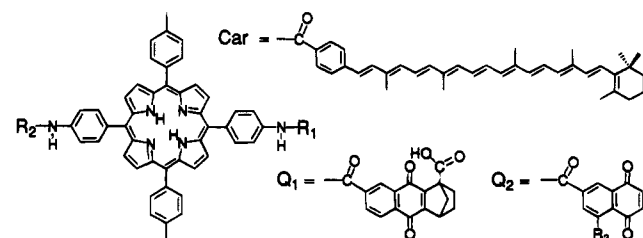


Figure 2. Decay of the C⁺ transient absorption at 950 nm in 1 and 2 following excitation of ~1 × 10⁻⁵ M solutions in benzonitrile with 10-ns, 650-nm laser pulses. Fits to exponential functions yield lifetimes of 233 ns and 2.5 μs for 1 and 62 ns for 2.

Chart 1



- | | | | |
|-----------------------------------|----------------------|-----------------------------------|----------------------|
| 1 R ₁ = Q ₁ | R ₂ = Car | 4 R ₁ = Q ₁ | R ₂ = -H |
| 2 R ₁ = Q ₂ | R ₂ = Car | 5 R ₁ = Q ₂ | R ₂ = -H |
| 3 R ₁ = Q ₂ | R ₂ = Car | 6 R ₁ = Q ₂ | R ₂ = -H |
| | R ₃ = -Cl | | R ₃ = -Cl |
| | R ₃ = -H | | R ₃ = -H |

designed as reference for the hydrogen-bonded form of triad 1. It incorporates the same P–Q (and C–P) linkages used in 1 and is assumed to have similar thermodynamics for the initial electron transfer step, based on the similarity of its photoinduced electron transfer rate in benzonitrile to that of the hydrogen-bonded form of 1.^{13,14} Electron transfer from C to P is essentially congruous in the two triads. Therefore, differences between 1 and 2 in the dynamics and quantum yields of subsequent transient species can be attributed to the proton transfer process in 1.

(10) The species with the shorter fluorescence lifetime is assigned to the hydrogen-bonded conformer, which has a greater driving force for electron transfer.

(11) Fluorescence lifetimes were determined by global analysis using the single photon timing method with excitation at 590 nm.¹²

(12) Gust, D.; Moore, T. A.; Luttrull, D. K.; Seely, G. R.; Bittersmann, E.; Bensasson, R. V.; Rougée, M.; Land, E. J.; De Schryver, F. C.; Van der Auweraer, M. *Photochem. Photobiol.* **1990**, *51*, 419–426.

(13) Marcus, R.; Sutin, N. *Biochim. Biophys. Acta* **1985**, *811*, 265–322.

(14) The driving force cannot be determined electrochemically because cyclic voltammetric measurements on 1 or appropriate model quinones report the potential for reduction of the quinone to the semiquinone. Because the first reduction potential of 1-carboxymethyl-1,2,3,4-tetrahydro-1,4-methanoanthracene-9,10-dione is 0.16 V more negative than that of the quinone moiety of 2 (and 5), the methyl ester derivative of the carboxylic acid in 1 is not an appropriate reference triad.

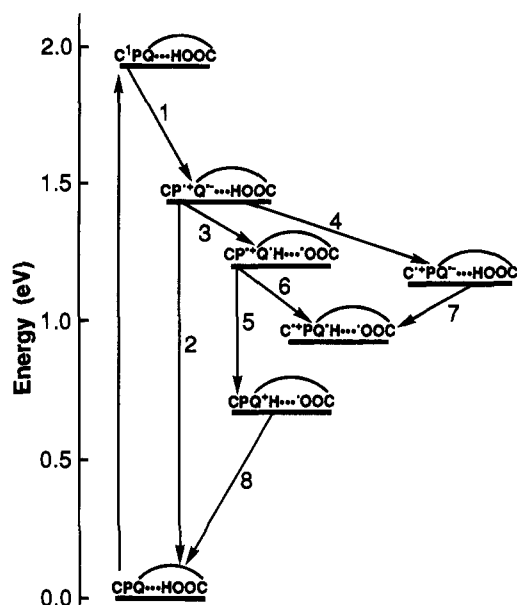


Figure 3. Transient states and related decay pathways for triad 1.

Information relevant to the states formed on excitation of **1** and **2** was obtained by directly probing the corresponding species in P–Q dyads **4–6** using transient absorption techniques. The spectra in the 624–766 nm region were characteristic of ^1P and P^{*+} ,^{2,15} and featured a rapid rise and slower decay. Global analysis of the decays gave time constants of 35, 33, and 121 ps for **4–6**, respectively, that are similar to those observed by fluorescence spectroscopy (43, 41, and 113 ps) and reflect the ^1P lifetimes. The rise times thus report the lifetimes of the porphyrin radical cation states, which are shorter than the formation times. These rise times are ~ 250 fs (the width of the excitation pulse) for model dyads **5** and **6** and represent upper limits for the lifetimes of $\text{P}^{*+}-\text{Q}^{\cdot-}$ (Figure 1a). The hydrogen-bonded dyad **4** exhibits a ~ 4 -ps rise time (Figure 1b).¹⁶ Thus, the P^{*+} state in **4** has a substantially longer lifetime than it does in the non-hydrogen-bonded analogs.

The quantum yields and lifetimes of the final charge-separated states in the triads were assessed by monitoring the transient carotenoid radical cation absorptions (Figure 2). The quantum yields¹⁷ of $\text{C}^{*+}-\text{P}-\text{Q}^{\cdot-}$ for **2** and **3** in benzonitrile were 0.10 and 0.11, and the corresponding lifetimes were 62 and 60 ns. For triad **1**, the yield¹⁸ was 0.22, and the carotenoid radical cation decayed on a much longer time scale.¹⁹ Triad **1** also had about twice the quantum yield of **2** and **3** in dichloromethane and in chloroform.

(15) Excitation was at 590 nm with ~ 200 -fs pulses.⁹

(16) The rise time for **4** was fit with exponential components of 350 fs and 3.8 ps. The 350-fs component is assigned to a combination of ^1P and the decay of P^{*+} in conformers lacking an intramolecular hydrogen bond, whereas the 3.8-ps component is attributed to the decay of P^{*+} in the hydrogen-bonded conformer.

(17) The quantum yields were calculated by the comparative method.¹

(18) This is the minimum quantum yield, as no correction has been made for the fraction of the triad in conformations lacking the intramolecular hydrogen bond.^{3,11}

(19) The decay of the transient absorption for **1** at 950 nm was fitted with exponentials of 233 ns and 2.5 μs . It is likely that the long-lived component involves bimolecular electron transfer reactions, and its decay is only approximated by an exponential.¹

(20) The energy of $\text{C}^{-1}\text{P}-\text{Q}^{\cdot-}\cdot\text{HOOC}$ was calculated to be 1.90 eV from spectral data. The energy level for $\text{C}-\text{P}^{*+}-\text{Q}^{\cdot-}\cdot\text{HOOC}$, 1.43 eV, was estimated from the cyclic voltammetric first oxidation potential of 5,15-bis(4-acetamidophenyl)-10,20-bis(4-methylphenyl)porphyrin (**7**) (0.89 V vs SCE in benzonitrile) and the first reduction potential of 5-chloro-7-phenylcarbamiyl-1,4-naphthoquinone (-0.54 V). This is the appropriate model quinone for this transient state.¹⁴ The energy level for $\text{C}-\text{P}^{*+}-\text{Q}^{\cdot-}\text{H}\cdot\cdot\text{OOC}$, 1.20 eV, was obtained from the first oxidation potential of **7** and the first reduction potential of 1-carboxy-6-phenylcarbamiyl-1,2,3,4-tetrahydro-1,4-methanoanthracene-9,10-dione (-0.31 V). The energy of $\text{C}-\text{P}-\text{Q}^{\cdot+}-\text{H}\cdot\cdot\text{OOC}$ (0.64 eV) was estimated using a $\text{p}K_a$ of -5.6 for the protonated quinone⁴ and a $\text{p}K_a$ of 5 for the carboxylic acid. The energies of the remaining charged species were estimated from the data above and the first oxidation potential of a carotenoid model compound (0.59 V).

Triad **1**, which demonstrates intramolecular hydrogen bonding, has substantially different transient properties than model triads **2** and **3**. The results are consistent with Figure 3.²⁰ Electron transfer from $\text{C}^{-1}\text{P}-\text{Q}^{\cdot-}\cdot\text{HOOC}$ yields $\text{C}-\text{P}^{*+}-\text{Q}^{\cdot-}\cdot\text{HOOC}$. Competing with charge recombination²¹ are steps **3** and **4**, which initiate electron transfer cascades that lead to the same final charge-separated state. Step **3** involves intramolecular proton transfer to the quinone anion radical to yield the semiquinone and the carboxylate anion ($\text{C}-\text{P}^{*+}-\text{Q}^{\cdot-}\text{H}\cdot\cdot\text{OOC}$, $k_3 \sim 1 \times 10^{12} \text{ s}^{-1}$). Recombination of this new state by step **5** gives $\text{C}-\text{P}-\text{Q}^{\cdot+}-\text{H}\cdot\cdot\text{OOC}$, which is a very energetic species due to the ~ 10.6 difference in $\text{p}K_a$ between the protonated quinone and carboxylic acid groups. Thus, the driving force for step **5** is much less than for step **2**, and k_5 is expected to be less than k_2 .²² Electron transfer from the carotenoid to yield the final $\text{C}^{*+}-\text{P}-\text{Q}^{\cdot-}\text{H}\cdot\cdot\text{OOC}$ state (step **6**) can therefore compete relatively well with charge recombination. Indeed, the efficiency of step **6** is high in **1**.²³ Step **4** also competes with recombination of the initial charge-separated state (step **2**) to give $\text{C}^{*+}-\text{P}-\text{Q}^{\cdot-}\cdot\text{HOOC}$, which can go on by proton transfer step **7** to yield the final charge-separated species.

The higher yield of the final charge-separated state in **1** relative to model compounds **2** and **3** is ascribed to pathways **3** and **6**, which compete favorably with recombination steps **2** and **5**. This interpretation is supported by the IR and fluorescence measurements, which indicate that a fraction of **1** exists in an intramolecularly hydrogen-bonded form.^{3,10,11} Addition of water, methanol, or benzoic acid to benzonitrile solutions of **1** increased the fluorescence lifetime of the major component from 51 to 70, 80, and 70 ps and decreased the yield of the final state from 0.22 to 0.11, 0.08, and 0.09, respectively. These changes are attributed to disruption of the internal hydrogen bond. Similar experiments with **2** or **3** did not change the fluorescence lifetime and increased the yield of $\text{C}^{*+}-\text{P}-\text{Q}^{\cdot-}$.²⁴

The results demonstrate that the yield of charge separation in multicomponent molecular photovoltaics can be increased by a coordinated electron and proton transfer process. It is also interesting that in **1** a substantial fraction of the intramolecular redox potential produced by photoinduced electron transfer is transformed into proton chemical potential. Elaboration of this concept could lead to photoinduced generation of proton motive force in a heterogeneous system.

Acknowledgment. This work was supported by a grant from the U.S. Department of Energy (DE-FG03-93ER14404) and the Petroleum Research Fund (23911 AC4).

JA943669C

(21) Rate constants for **1** in benzonitrile have been estimated for the processes depicted in Figure 3. The quantum yield of step **1** was ~ 1 in all cases, and $k_1 = 2 \times 10^{10} \text{ s}^{-1}$ based on the fluorescence lifetime of **1**. The lower limit for k_2 , $4 \times 10^{12} \text{ s}^{-1}$, was obtained from the lifetime of P^{*+} measured in model dyad **5** (see Figure 1a). Similarly, k_5 was estimated as $\sim 3 \times 10^{11} \text{ s}^{-1}$ from the lifetime of P^{*+} in dyad **4** (see Figure 1b). Steps **4** and **6** both involve electron donation by the carotenoid to P^{*+} , and to a first approximation, $k_4 = k_6 \geq 5 \times 10^{11} \text{ s}^{-1}$, estimated from k_2 and the quantum yield of $\text{C}^{*+}-\text{P}-\text{Q}^{\cdot-}$ in **2**. From a simplified quantum yield expression for **1**, $\Phi(\text{C}^{*+}-\text{P}-\text{Q}^{\cdot-}\text{H}\cdot\cdot\text{OOC}) = 0.22 \approx k_4/(k_4 + k_3 + k_2) + \{k_3/(k_4 + k_3 + k_2)\}\{k_6/(k_6 + k_5)\}$, the proton transfer rate constant, k_3 , was calculated to be $\sim 1 \times 10^{12} \text{ s}^{-1}$. Allowing only 70% of **1** to be in the hydrogen-bonded form yields $k_3 \sim 2 \times 10^{12} \text{ s}^{-1}$.¹⁸ For examples of intramolecular proton transfer reaction rates of the same order as k_3 , see: Formosinho, S. J.; Arnaut, L. G. *J. Photochem. Photobiol. A: Chem.* **1993**, *75*, 21–48 and references therein.

(22) Assuming a reorganization energy of ~ 1 eV, proton transfer shifts recombination from a faster rate in the Marcus inverted region (step **2**) to a slower rate in the normal region (step **5**).

(23) The yield of pathway **6** in Figure 3 is 0.6 in **1**, and the yield of the pathway analogous to **6** in **2** is 0.11. The yields for pathways **3** and **4** are 0.2 and 0.09, respectively, calculated from the relevant rate constants.²¹

(24) The triad concentrations were $\sim 1 \times 10^{-5}$ M in benzonitrile, methanol concentrations were 0.1–1 M, water concentrations were 0.1–0.3 M, and benzoic acid concentrations were 0.5×10^{-5} – 1×10^{-4} M. The yield of $\text{C}^{*+}-\text{P}-\text{Q}^{\cdot-}$ in the case of **2** in benzonitrile/1 M methanol was 20%, and for **3** in benzonitrile/0.3 M water it was 17%.